

## Main-Chain Smectic Liquid Crystalline Polymer Exhibiting Unusually High Thermal Conductivity in an Isotropic Composite

Shusuke Yoshihara,<sup>1,2</sup> Masatoshi Tokita,<sup>2</sup> Toshiaki Ezaki,<sup>1</sup> Mitsuru Nakamura,<sup>1</sup> Masashi Sakaguchi,<sup>1</sup> Kazuaki Matsumoto,<sup>1</sup> Junji Watanabe<sup>2</sup>

<sup>1</sup>Frontier Materials Development Laboratories, Kaneka Corporation 5-1-1, Torikai-Nishi, Settsu, Osaka 566-0072, Japan

<sup>2</sup>Department of Organic and Polymeric Materials, Tokyo Institute of Technology, 2-12-1, Ookayama, Meguro-ku, Tokyo 152-8552, Japan

Correspondence to: S. Yoshihara (E-mail: Shusuke\_Yoshihara@kn.kaneka.co.jp)

**ABSTRACT:** The thermal conductivity (TC) of an isotropic composite comprising of a main-chain smectic liquid crystalline PB-10 polyester and 50- $\mu\text{m}$ -sized roughly spherical magnesium oxide (MgO) particles is investigated. The increase in the composite TC with higher MgO fractions is steeper than that expected by Bruggeman's theory for the TC of a polydomain PB-10 polyester ( $0.52 \text{ W m}^{-1} \text{ K}^{-1}$ ). When the filler content is larger than 30 vol %, the composite TC approaches a value that can be explained only if the polyester functions as a matrix with  $1.0 \text{ W m}^{-1} \text{ K}^{-1}$ , which is five times as high as those of isotropic common polymers ( $0.2 \text{ W m}^{-1} \text{ K}^{-1}$ ). Such an unusually high TC for a polymer matrix is attributed to some polymer lamellae that lie parallel to the particle surface and are stacked toward neighboring particles, thus creating effective heat paths between the particles and a continuous thermal network in a composite. © 2013 Wiley Periodicals, Inc. *J. Appl. Polym. Sci.* **2014**, *131*, 39896.

**KEYWORDS:** composites; liquid crystals; morphology; polyesters; thermal properties

Received 13 June 2013; accepted 22 August 2013

DOI: 10.1002/app.39896

### INTRODUCTION

Thermally conductive, electrically insulating materials have attracted attention as useful substances for heat dissipation in electronic devices. The improvement of devices in size and performance results in the generation of a greater amount of heat in a smaller volume of space. To remove the heat, materials with higher thermal conductivity (TC) are demanded. Polymers are lightweight electrical insulators; however, their TC is typically very low ( $0.1\text{--}0.5 \text{ W m}^{-1} \text{ K}^{-1}$ ).<sup>1–3</sup> Even with large concentrations of thermally conductive fillers, it is difficult to enhance the polymer composite TC because the polymer matrix plays a major role in the heat transfer process.<sup>4–6</sup> Moreover, a high filler content leads to undesirable weight gain and poor processability. A possible solution to solve these issues is to enhance the polymer matrix TC. The TC of polymer composites can be significantly increased when the polymer matrices serve as good heat conductors between the filler particles.<sup>5,6</sup> High density polyethylene (HDPE) exhibits the highest TC value (ca.  $0.5 \text{ W m}^{-1} \text{ K}^{-1}$ ) of common thermoplastics.<sup>3</sup> To the best of our knowledge, cured resins of phenyl benzoate twin mesogen-type bisepoxide compounds with

4,4'-methylenedianiline exhibit the highest TC ( $0.85\text{--}0.96 \text{ W m}^{-1} \text{ K}^{-1}$ ) of all isotropic polymer materials.<sup>7</sup> Therefore, other thermally conductive polymer matrices are being investigated with the immediate aim of increasing the TC to more than  $1 \text{ W m}^{-1} \text{ K}^{-1}$ .

Previously, we found that main-chain smectic liquid crystalline (LC) PB-10 polyester acted as a thermally conductive matrix in composites.<sup>8</sup> The PB-10 polyester, consisting of 1,10-dodecanedioic acid and 4,4'-biphenol [Figure 1(a)], forms a smectic I LC phase in which 2-nm-length polymer repeat units are accommodated in monoclinic lattices with a very extended conformation.<sup>9</sup> At a larger length scale, 47-nm-thick lamellae with large lateral dimensions regularly stack along the polymer chain direction [Figure 1(b)].<sup>8–12</sup> Injection molding of the PB-10 polyester in the LC state aligned the lamella normal in the normal direction (ND) with respect to the molding surface, thus leading to a high TC ( $1.2 \text{ W m}^{-1} \text{ K}^{-1}$ ) in the direction.<sup>8</sup> Such a lamellar orientation was also observed in injection-molded PB-10 composites with plate-shaped hexagonal boron nitride (h-BN), where both the h-BN plates and the polymer lamellae aligned with their normal in the ND. Increasing the

Additional Supporting Information may be found in the online version of this article.

© 2013 Wiley Periodicals, Inc.

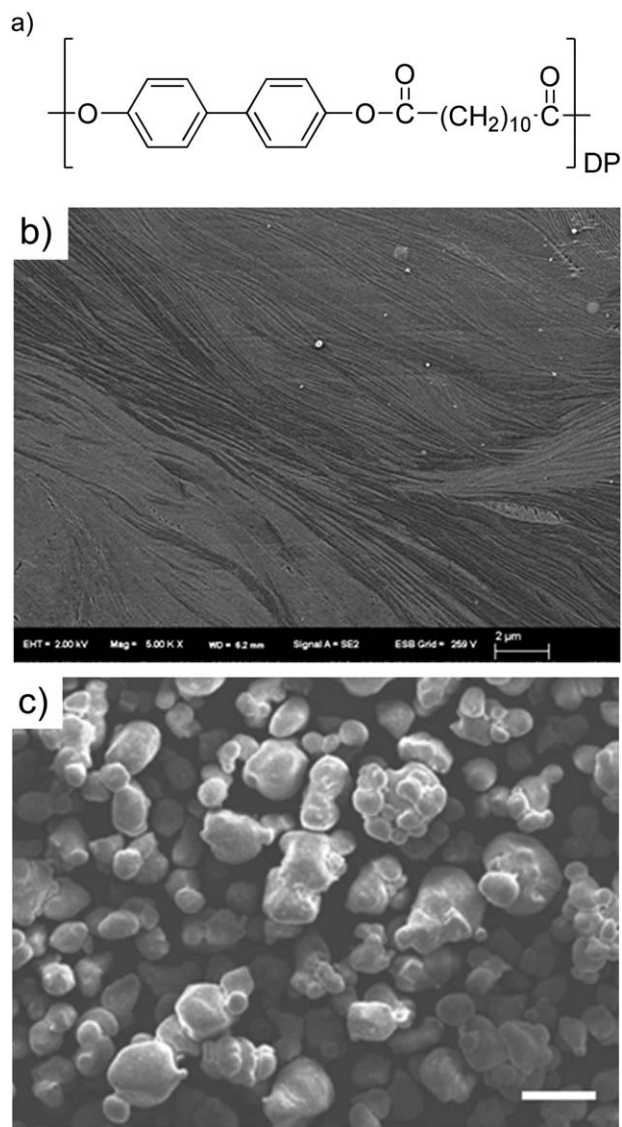


**Figure 1.** Components of the polymer composite: (a) Chemical structure of PB-10. (b) SEM image of the lamellae of PB-10. Scale bar: 2  $\mu\text{m}$ . (c) fsSEM image of the MgO particles. Scale bar: 50  $\mu\text{m}$ .

h-BN content significantly enhanced the TC in the in-plane direction (ID) as well as in the ND, indicating that the polymer lamellae served as effective heat paths between the h-BN platelets.

Herein, we examined the TC of PB-10 composites with magnesium oxide (MgO) roughly spherical particles with a mean size of 50  $\mu\text{m}$  [Figure 1(c)]. The compression-molded composites at more than 30 vol % exhibited much larger TC than that expected by Bruggeman's theory for the TC of the polydomain PB-10 matrix. Moreover, these results indicated that the polydomain PB-10 polyester with only 0.52  $\text{W m}^{-1} \text{K}^{-1}$  functioned as an isotropic matrix with 1  $\text{W m}^{-1} \text{K}^{-1}$ . Such an unexpectedly high TC value is attributed to the polymer lamellae that lie parallel to the particle surface and are stacked between the particles, thus serving as heat paths between the MgO particles.

## EXPERIMENTAL

### Materials

PB-10 polyester [Figure 1(a)] was synthesized by melt condensation of 4,4'-diacetoxy biphenyl and 1,10-dodecanedioic acid with sodium acetate as the catalyst. The number average molecular weight ( $M_n$ ) and polydispersity index of the polymer were determined by gel permeation chromatography (GPC) in a *p*-chlorophenol/toluene (3/8 volume ratio) solution using polystyrene standards (Viscotek Ht-GPC with an RI detector) to be  $2.4 \times 10^4$  and 2.4, respectively. The crystal-smectic and smectic-isotropic phase transition temperatures of the polymer were  $T_m = 206^\circ\text{C}$  and  $T_i = 256^\circ\text{C}$ , respectively, as determined by differential scanning calorimetry (DSC) at a heating rate of  $10^\circ\text{C min}^{-1}$  (Perkin Elmer Pyris 1 DSC, Figure S1, Supporting Information).

The composites were prepared by mixing PB-10 with MgO particles with a mean particle size of 50  $\mu\text{m}$  (Ube Materials RF-50-SC, treated the surfaces by vinylmethylsiloxane homopolymer) at  $220^\circ\text{C}$  using a TECHNOVEL KZW15TW twin-screw extruder at a screw rotation speed of 90 rpm. The MgO content was determined by the composite density and residual content after a burn-out test at  $450^\circ\text{C}$ . The polymer and composites were molded via compression molding at  $270^\circ\text{C}$  for 3 min (Toyoseiki mini test press-10) to shape them into plates that were 25.4 mm in diameter and 1 mm in thickness. The plates were then cooled to 25 at  $50^\circ\text{C min}^{-1}$ .

### Measurements

The TC ( $\lambda$ ) of the samples was calculated using eq. (1) and the results of density ( $\rho$ ), heat capacity ( $C_p$ ), and thermal diffusivity ( $\alpha$ ) measurements:

$$\lambda = \alpha \rho C_p. \quad (1)$$

The  $\alpha$  was measured in triplicate at  $25^\circ\text{C}$  in accordance with the American Society for Testing and Materials E-1461 using a Netzsch LFA 447 NanoFlash with an accuracy of  $\pm 5\%$  (Figure S2, Supporting Information). The  $\rho$  and  $C_p$  were determined using the Archimedes and DSC methods, respectively.

Scanning electron microscope (SEM) observations were conducted using a Hitachi S-4800 SEM. To observe the dispersion of MgO particles in composites, each specimen with the surface polished with sandpaper was subjected to platinum–palladium deposition. To observe the crystalline lamellae of PB-10, the specimen with the surface smoothed using a microtome was exposed to  $\text{RuO}_4$  vapor before platinum–palladium deposition. Polarizing optical microscopy (POM) was performed using an Olympus B-50 microscopy with an inserted 530-nm sensitive tint plate. To observe the polymer domains in a composite, the specimen was adhered to a glass slide and thinned to about 2  $\mu\text{m}$  with sandpaper.

## RESULTS AND DISCUSSION

PB-10 composites with MgO fractions ranging from 0 to 37 vol % were prepared. Figure 2(a,b) show the SEM images observed on a polished surface of the composites at 9 and 29 vol %, respectively, indicating that MgO particles are randomly

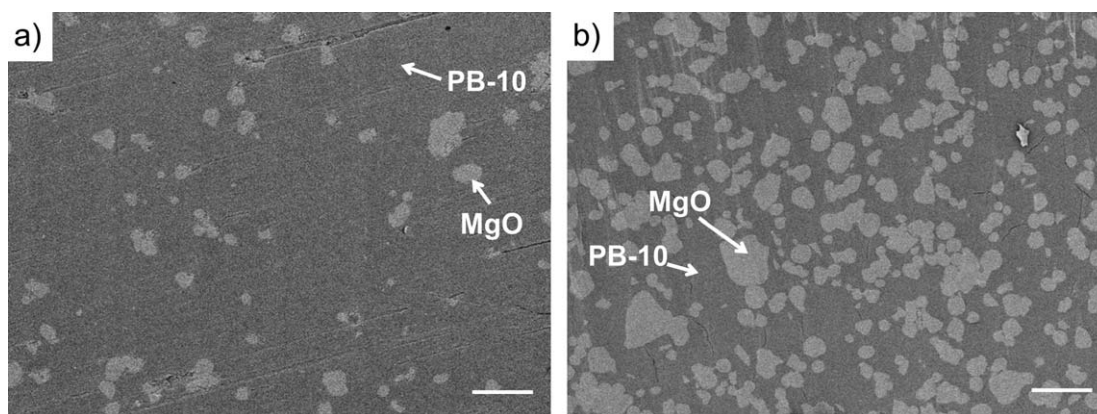


**Figure 2.** SEM images of the polished surface for PB-10 composites. (a) 9 vol % and (b) 29 vol %. Scale bar: 100  $\mu\text{m}$ .

distributed and the interface between polymer matrix and particles appears to be continuous without voids. The detailed values of the  $\lambda$ ,  $\alpha$ ,  $\rho$ , and  $C_p$  for all composites in this study are summarized in Table S1 (Supporting Information). Figure 3 shows the TC of the composites in the ND and ID as a function of the volume fraction of MgO ( $\nu$ ) compared with the theoretical curves calculated using Bruggeman's equation<sup>13</sup>:

$$1 - \nu = \frac{\lambda_1 - \lambda_3}{\lambda_2 - \lambda_3} \left( \frac{\lambda_2}{\lambda_1} \right)^{1/3}, \quad (2)$$

where  $\lambda_1$ ,  $\lambda_2$ , and  $\lambda_3$  are the TCs of the composite, polymer matrix, and MgO ( $42 \text{ W m}^{-1} \text{ K}^{-1}$ ),<sup>14</sup> respectively. Bruggeman model was based on spherical particles homogeneously suspended in a matrix, similar to composites in this study. Generally, it is known that experimental values are in agreement with those predicted by this equation at low filler content ( $< 40 \text{ vol } \%$ ).<sup>15–17</sup> Therefore, composites at up to 40 vol % loading are discussed here. The solid and broken lines in Figure 3 represent

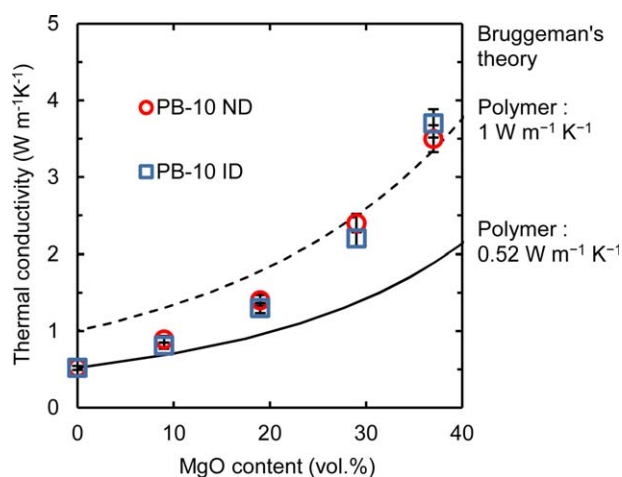


**Figure 3.** Effect of MgO filler content on the TC of compression-molded PB-10 composites compared with the theoretical curves calculated using Bruggeman's equation. The solid and broken lines represent the calculated  $\lambda_1$  values with  $(\lambda_2, \lambda_3) = (0.52, 42)$  and  $(1, 42)$ , respectively. [Color figure can be viewed in the online issue, which is available at [wileyonlinelibrary.com](http://wileyonlinelibrary.com).]

the calculated  $\lambda_1$  values with  $\lambda_2 = 0.52$  and  $1 \text{ W m}^{-1} \text{ K}^{-1}$ , respectively. The value of  $0.52 \text{ W m}^{-1} \text{ K}^{-1}$  is equal to the experimental TC value of the pure polydomain PB-10. The TCs in the ND and ID are similar, indicating that the composites are isotropic. It is interesting to note that the increase in the TC of the composites is steeper than that of the solid line curve in Figure 3. In contrast, the TC of HDPE/MgO and polycarbonate/MgO composites with the same MgO fraction range are well explained by the same equation (Figure S3, Supporting Information). Thus, such an anomalous increase in the PB-10 composite TC cannot be ascribed to the percolation effects that are remarkable at  $\nu > 50 \text{ vol } \%$ .<sup>18,19</sup> In addition, the crystallinity of the polymer matrix in each composite was estimated from the transition enthalpy ( $\Delta H$ ) value per unit weight of polymer at  $T_m$  and  $T_i$  in an attempt to account for the steep TC enhancement. However, the enthalpy changes were nearly constant, irrespective of the MgO content (Table S2, Supporting Information). Thus, such an increase in the TC of the PB-10 composite is entirely unexpected.

Such a high TC can, however, be ascribed to polymer lamellar stacking between the MgO particles. Figure 4 shows SEM images of the composite at an MgO fraction of 9 vol %. Between the MgO particles at a greater distance, the lamellae stack in various directions [Figure 4(a)]. However, between the filler particles at a shorter distance ( $\sim 5 \mu\text{m}$ ), some lamellae lie parallel to the surfaces of the MgO particles and are regularly stacked toward the surface of the neighboring MgO sphere [Figure 4(b)]. These lamellae can serve as heat paths between the MgO particles; the TC is estimated to be  $> 1 \text{ W m}^{-1} \text{ K}^{-1}$ , because the injection-molded PB-10 exhibits a TC of  $1.2 \text{ W m}^{-1} \text{ K}^{-1}$  along the lamellar stacking direction.<sup>8</sup> In fact, the TC of the PB-10 composites asymptotically approaches the broken line curve with  $\lambda_2 = 1 \text{ W m}^{-1} \text{ K}^{-1}$  in Figure 3, suggesting that the matrix TC gradually increases from  $0.52$  to  $1 \text{ W m}^{-1} \text{ K}^{-1}$  with the increase in MgO fractions.

Such regular polymer lamellar stacking is thought to be achieved when the dimensions of the gap between the MgO particles decreases and becomes comparable to the coherence length of the polymer lamellar stacking. The coherence length of PB-10 lamellar stacking can be as large as  $20 \mu\text{m}$ . Figure 5



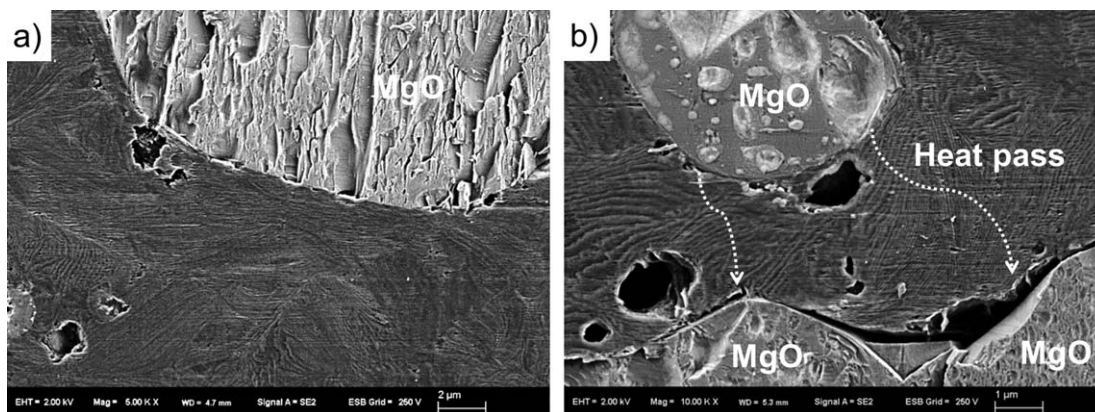


**Figure 4.** SEM images of a compression-molded PB-10/MgO composite at 9 vol % loading. (a) A large gap between the MgO particles. Scale bar: 2  $\mu\text{m}$ . (b) A small gap between the MgO particles. Scale bar: 1  $\mu\text{m}$ .

shows a POM image of a PB-10 thin film microtomed from a bulk polymer (thickness: 500 nm). The blue domains are due to an increase in the retardation of the uniaxially oriented domain and the sensitive tint plate (530 nm) resulting from the alignment of the chain axis direction with the  $Z$  direction. Therefore, the lamellae are stacked along the polymer chain direction in length from a few micrometers to about 20  $\mu\text{m}$ . In addition, the anisotropic domain is expected to have high TC of  $1 \text{ W m}^{-1} \text{ K}^{-1}$  along the lamellar stacking direction and only modest at  $0.30 \text{ W m}^{-1} \text{ K}^{-1}$  in the perpendicular direction. The disorderly oriented domains and the domain boundaries cause phonon scattering, leading to the polydomain TC value of  $0.52 \text{ W m}^{-1} \text{ K}^{-1}$ . However, the distance between the filler particles decreases with the increase in filler fractions as seen in Figure 2(a,b). The mean distance can be calculated as 47.5  $\mu\text{m}$  at 10 vol % and decreases to 17.6  $\mu\text{m}$  at 30 vol %, assuming a face-centered cubic lattice model (Figure 6). Thus, the amount of disordered domains and domain boundaries in the interparticle gap decreases. This is thought to result in the gradual increase of matrix TC as the MgO content increases. The matrix TC values ( $\lambda_2$ ) at 9 and 19 vol % can be calculated from the

composite TC values in Figure 3 using Bruggeman's eq. (2) to be 0.65 and  $0.75 \text{ W m}^{-1} \text{ K}^{-1}$ , respectively. At around 30 vol %, all particles are arranged near to each other [Figure 2(b)]. Figure 7 shows a POM image of the composite film (29 vol %) prepared from the mold using sandpaper (thickness: about 2  $\mu\text{m}$ ). The image indicates that the interparticle gaps within 20

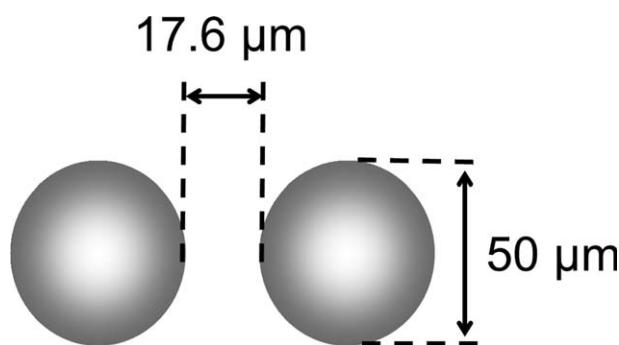


**Figure 6.** Theoretical distance between 50- $\mu\text{m}$  MgO particles at 30 vol % loading.

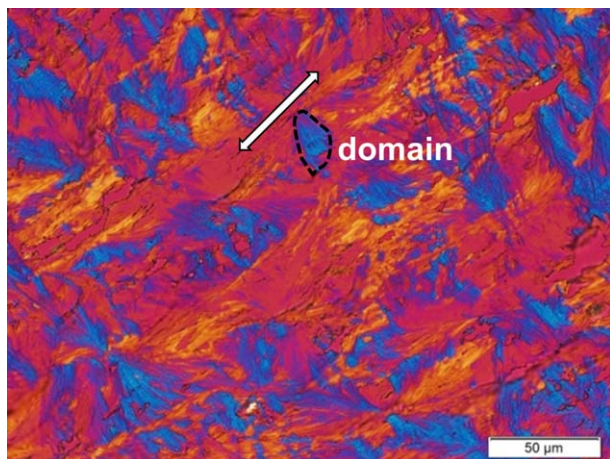


**Figure 5.** POM image of a PB-10 thin film (500 nm). The double-headed arrow shows the  $Z$  direction of the 530-nm sensitive tint plate. Scale bar: 50  $\mu\text{m}$ . [Color figure can be viewed in the online issue, which is available at wileyonlinelibrary.com.]

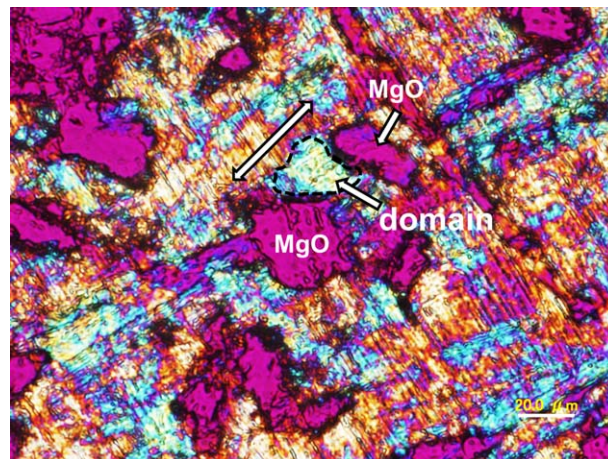


**Figure 7.** POM image of a PB-10/MgO composite thin film (about 2  $\mu\text{m}$ ) at 29 vol % loading. The double-headed arrow shows the  $Z$  direction of the 530-nm sensitive tint plate. Scale bar: 20  $\mu\text{m}$ . [Color figure can be viewed in the online issue, which is available at wileyonlinelibrary.com.]

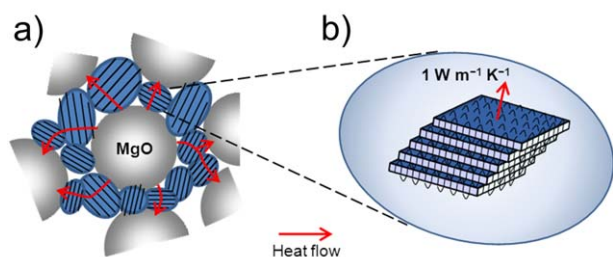


**Figure 8.** Schematic illustration of the structural model for TC enhancement of PB-10/MgO composites at high MgO particle loadings. (a) Heat conduction between the MgO particles via the crystal domain of PB-10. (b) Laterally large and well-stacked lamellar crystals with more than  $1 \text{ W m}^{-1} \text{ K}^{-1}$  heat conduction along the chain direction. [Color figure can be viewed in the online issue, which is available at [wileyonlinelibrary.com](http://wileyonlinelibrary.com).]

$\mu\text{m}$  are filled by one or a few domains with lamellar normal connecting the filler surfaces. Such domains can serve as effective heat paths between the MgO particles as depicted schematically in Figure 8, and create a continuous thermal network in composites. Consequently, the TC of the PB-10 matrix ( $\lambda_2$ ) becomes  $1 \text{ W m}^{-1} \text{ K}^{-1}$ .

Above filler concentration of 30 vol %, the polydomain PB-10 polyester can be used as a matrix with a TC of  $1.0 \text{ W m}^{-1} \text{ K}^{-1}$ , which is five times as high as those of isotropic common polymers; without fillers, it has a TC as high as  $0.52 \text{ W m}^{-1} \text{ K}^{-1}$ . To attain a composite TC of  $2 \text{ W m}^{-1} \text{ K}^{-1}$ , which is 10 times higher than those of common polymers, PB-10 requires an amount of MgO that is 20 vol % lower than that required for other common polymers with TC values of  $0.25 \text{ W m}^{-1} \text{ K}^{-1}$  (Figure 2 and S3 in the Supporting Information). As a result, lighter weight composites with good processability can be prepared using PB-10. It is still difficult to enhance the TC of an isotropic polymer itself to the level of  $1 \text{ W m}^{-1} \text{ K}^{-1}$ . However, a polymer matrix with a TC of  $1 \text{ W m}^{-1} \text{ K}^{-1}$  is obtainable using the current technique.

## CONCLUSIONS

Polydomain LC PB-10 polyester serves as a heat path with a TC of  $1.0 \text{ W m}^{-1} \text{ K}^{-1}$  in composites at 50- $\mu\text{m}$ -sized MgO content of more than 30 vol %, although the TC of the polydomain is  $0.52 \text{ W m}^{-1} \text{ K}^{-1}$ . Such a high TC value of the polymer matrix is ascribed to the fact that the polymer lamellae are stacked at a coherence length of micron order and exhibit a TC of  $1.0 \text{ W m}^{-1} \text{ K}^{-1}$  in the ND. When the MgO content is more than 30 vol %, some polymer lamellae lying parallel to the MgO particles can stack toward neighboring MgO spheres and a

continuous thermal network is created in composites. Thus, a polymer with a TC of only  $0.52 \text{ W m}^{-1} \text{ K}^{-1}$  functions as a thermally conductive matrix with a TC as large as  $1 \text{ W m}^{-1} \text{ K}^{-1}$ .

## ACKNOWLEDGMENTS

This work was partially supported by the New Energy and Industrial Technology Development Organization (NEDO). The authors thank Masayuki Honda at Kaneka Techno Research for assisting with the POM and SEM observations.

## REFERENCES

- Han, Z.; Fina, A. *Prog. Polym. Sci.* **2011**, *36*, 914.
- Choy, C. L.; Ong, E. L.; Chen, F. C. *J. Appl. Polym. Sci.* **1981**, *26*, 2325.
- Hansen, D.; Bernier, G. A. *Polym. Eng. Sci.* **1972**, *12*, 204.
- Wattanukul, K.; Manuspiya, H.; Yanumet, N. *J. Compos. Mater.* **2010**, *45*, 1967.
- Mamunya, E. P.; Davydenko, V. V.; Pissis, P.; Lebedev, E. V. *Eur. Polym. J.* **2002**, *38*, 1887.
- Sundstrom, D. W.; Lee, Y.-D. *J. Appl. Polym. Sci.* **1972**, *16*, 3159.
- Akatsuka, M.; Takezawa, Y. *J. Appl. Polym. Sci.* **2003**, *89*, 2464.
- Yoshihara, S.; Ezaki, T.; Nakamura, M.; Watanabe, J.; Matsumoto, K. *Macromol. Chem. Phys.* **2012**, *213*, 2213.
- Tokita, M.; Okuda, S.; Yoshihara, S.; Takahashi, C.; Kang, S.; Sakajiri, K.; Watanabe, J. *Polymer* **2012**, *53*, 5596.
- Asrar, J.; Toriumi, H.; Watanabe, J.; Krigbaum, W. R.; Ciferri, A. *J. Polym. Sci. Polym. Phys. Ed.* **1983**, *21*, 1119.
- Krigbaum, W. R.; Watanabe, J.; Ishikawa, T. *Macromolecules* **1983**, *16*, 1271.
- Tokita, M.; Osada, K.; Yamada, M.; Watanabe, J. *Macromolecules* **1998**, *31*, 8590.
- Bruggeman, D. A. G. *Ann. Phys.* **1935**, *24*, 636.
- Jeong, I.; Kim, J.; Lee, J.; Hong, J. *Trans. Electr. Electron. Mater.* **2010**, *11*, 261.
- Teng, C.-C.; Ma, C.-C. M.; Chiou, K.-C.; Lee, T.-M. *Compos. B* **2012**, *43*, 265.
- Wong, C. P.; Bollampally, R. S. *J. Appl. Polym. Sci.* **1999**, *74*, 3396.
- Yorifuji, D.; Ando, S. *J. Mater. Chem.* **2011**, *21*, 4402.
- Monden, K. *Adv. Sci. Technol.* **2006**, *45*, 2664.
- Bigg, D. M. *Adv. Polym. Sci.* **1995**, *119*, 1.